JOURNAL OF MATERIALS SCIENCE 25 (1990) 3605–3610

Critical values of stress intensity factor in mode II fracture of cementitious composites

A. M. BRANDT
Institute of Fundamental Technological Research, Polish Academy of Sciences, 00-049 Warszawa, Swiętokrzyska 21, Poland

G. PROKOPSKI
Technical University, 42-200 Częstochowa, Zawadzkiego 27, Poland

The problem of mode II of brittle matrix composites is considered. After a short discussion of the present knowledge and a review of test results, the importance of fracture toughness in mode II is stressed. The test results presented concern both modes of fracture, and obtained values of stress intensity factors K_{Ic} and K_{IIc} are discussed, taking into consideration the results of observations on SEM micrographs. It is suggested that the fracture toughness of concrete-like materials should be expressed as a combination of mode I and II characteristics.

1. Introduction

The application of fracture mechanics to the large group of cement-based materials, following the earliest papers by Kaplan [1] and Glücklich [2], has led to many interesting results. Experimental data on the principal parameters according to both linear and non-linear fracture mechanics have been published, together with discussions on the validity of both these approaches. The large majority of these studies concerned mode I of fracture. However, the importance of modes II and III should not be underestimated, particularly for highly heterogeneous materials like cement mortars and concretes.

In this paper some arguments for also applying mode II are proposed, together with a short review of the critical values of the stress intensity factor K_{IIc} obtained by various authors. New comparative test results on K_{IIc} are also presented.

2. The mixed-mode fracture

In a mixed-mode loading, when not only axial loading but also shearing is applied, it is assumed that fracture occurs when a total energy release rate, G, is larger than an energy consumption rate, R, and the fracture condition is given by $G \geqslant R$ [3]. The total energy release rate, G, for a linear elastic material is

$$G = G_I + G_{II} + G_{III} = \frac{(1 - \nu^2)}{E}(K_I^2 + K_{II}^2 + K_{III}^2) \quad (1)$$

For I to II mixed-mode loading, which may be adopted for the plane strain state, $K_{III} = 0$. This situation occurs in most cases when the dimensions of a loaded element admit the plane strain state. Therefore

$$G = \frac{(1 - \nu^2)}{E}(K_I^2 + K_{II}^2) \quad (2)$$

where E = Young's modulus and ν = Poisson's ratio.

If the above formula is simplified to the form

$$G = \frac{(1 - \nu^2)}{E} K_I^2 \quad (3)$$

as in nearly all published studies, it means that one of the following assumptions is accepted:

(i) the material under consideration is characterized by $K_{II} = 0$; or

(ii) the mode II of fracture does not exist at all in the fracture process considered.

Assumption (i) cannot be proved for any structural material, independently of whether its behaviour is considered as linear and elastic or non-linear and plastic, the fluids and gels being here excluded from the considerations. Assumption (ii) may be adopted for ideally homogeneous materials subjected to tensile loading. Its application to concrete-like materials seems inappropriate because of the high level of inhomogeneity. Even in the case of an ideal external loading, the local effects between grains and voids produce all three modes of fracture. The assumption that mode III may be neglected in a plane-strain state is more admissible.

Various experimental studies (for example, [4]) have shown that the cracks start from the mortar–aggregate grain interface. Crack propagation takes the form of a large amount of branching micro-cracks, leading sometimes to multiple macrocracking. Excellent examples of such crack patterns are given by Mindess [5] and similar patterns may be seen in every concrete element, even if the external load is applied as an ideal tension. Regarding these crack patterns, as well as their model representation [6], it is difficult to admit that the crack propagation is limited to mode I.

Two examples of possible mode II fracture in local situations around initial cracks or regions with different rigidity are shown in the form of an initial crack or flaw in the matrix (Fig. 1a) or of a bond crack along the surface of an aggregate grain (Fig. 1b). The nature of the external load–tension or compression – does

0022–2461/90 $03.00 + .12

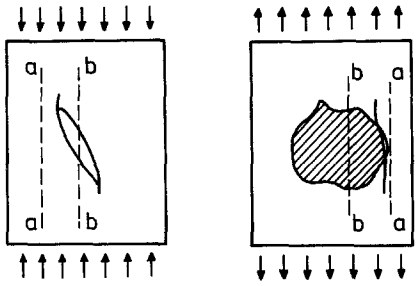

Figure 1 Local non-homogeneities as source of mode II fracture.

not modify these possibilities. The deformations along lines a–a and b–b are different in such a way that the in-plane shearing appears at the tips of initial notches and the mode II fracture is started.

Interesting results for the mixed mode fracture were observed by Debicki [7] from tests of transversally orthotropic fibre-reinforced mortar cylinders of 80 × 160 mm, subjected to axial compression. The compressive force P was applied at different angles (θ) with respect to the casting direction 1–1 (Fig. 2). The author used two different criteria for different regions of angle and obtained excellent experimental confirmation. For the angle θ between 0° and 45° and between 75° and 90°, the splitting of the cylinder under compression was decisive. For the angle θ between 45° and 75°, the shearing mode appeared because of weaker resistance against tangent stresses along layers perpendicular to the casting direction.

Combined loading which produces the mixed mode of cracking was considered by Broek [3] and two examples of fracture criteria were proposed:

$$K_{Ic}^2 + K_{IIc}^2 = K_c^2 \tag{4}$$

where it is assumed that $K_{Ic} = K_{IIc}$, and

$$(K_I/K_{Ic})^2 + (K_{II}/K_{IIc})^2 = 1, \quad \text{where } K_{Ic} \neq K_{IIc} \tag{5}$$

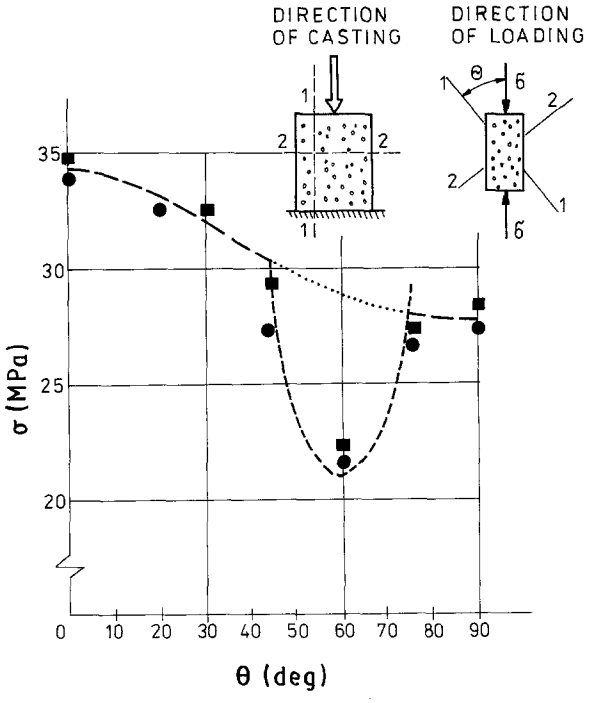

Figure 2 Results of compression tests: strength against angle θ. Experimental results compared with calculation according to two strength criteria [17]. (——) Tsai-Wu criterion; (– – –) Coulomb criterion. ●, ■, Experimental results for two series of specimens.

For the second of these criteria, it was assumed that the crack propagated in a self-similar manner and remained in the plane of the original crack. In experiments it is usually observed that a crack extends along an angle with respect to its original direction.

Some calculations given by Sih [8] or by Williams and Ewing [9], and repeated by Broek [3], show various attempts to deal with the mixed-mode fracture. Later Sih proposed certain criteria for mixed-mode fracture in isotropic and anisotropic materials taking into account the elastic energy in the neighbourhood of the tip of a notch [10, 11]. According to these criteria, a crack is initiated along a direction corresponding to the minimum of the strain energy density and when that minimum reaches a critical value. However, the relations proposed by Sih do not account for internal reinforcement like fibres or fabrics.

According to the formulae proposed by Hahn [12] and R'Mili [13], the fracture criterion for mixed mode is also based on the expression of global energy $G(K_I, K_{II})$ and its critical value G_c.

In heterogeneous and anisotropic materials like concretes, the problem should be considered in a different and more complicated way. It is not a single crack subjected simultaneously to tension and in-plane shearing which produces a mixed mode of fracture, but a spectrum of loading conditions which produce various mixed modes of fracture. In that spectrum modes I and II are the only limiting case, all others are the different combinations of both of them.

A model may be therefore proposed in which critical values of K_{Ic} and K_{IIc} both determine a critical value of an overall factor K_c, being a measure for the material crack resistance. This was presented by Sih *et al.* [10] as a function describing a critical state:

$$f(K_{Ic}, K_{IIc}) = f_c \tag{6}$$

without defining any particular form of that function.

One of the possible ways to find an acceptable form of the function (6) is to execute a series of experiments in which materials of known K_{Ic} and K_{IIc} will be combined. Different proportions of both materials and carefully arranged macro-regions in a tested element may help to determine the practically reliable function $f(K_{Ic}, K_{IIc})$. The high degree of indeterminacy of the system which represents a concrete specimen may make such a problem quite difficult to deal with.

Any attempt to solve the above formulated problem should be initiated by determination of the K_{IIc} values for concrete-like materials.

3. Values of K_{IIc} determined by various authors

Tests in which the values of K_{IIc} were measured are not very numerous, but all available data are shown in Table I. They concern different concretes with variable composition. The data from different authors are not very dispersed, which may be explained by a similar method of testing adopted by all authors. In most cases the higher values of K_{IIc} correspond to the materials for which higher strength and a better aggregate–matrix bond were also observed or may be supposed, if the appropriate data are not given. This

is expected, and reflects to some extent the material resistance against shearing crack propagation.

In the tests analysed in Table I, neither data for K_{Ic} nor information on the material strength and internal structure are available. Therefore an analysis of the data is limited. In such a situation a new series of tests was executed in which more complex data were looked for. These tests are described below.

4. Description of the tests

The specimens for determining separately the fracture properties for both modes I and II are shown in Figs 3 and 4. The specimens were cast with ordinary Portland cement, a fine aggregate of local deposit and river gravel with a maximum grain size of 10 mm. The following compositions were used:

Concrete 1 : 1.9 : 3.2 : 0.5 (cement : fine aggregate : coarse aggregate : water)
Mortar 1 : 2.0 : 0.4
Paste 1 : 0.26

All mixes were prepared in a pan mixer and a vibrating table was used for compaction. The specimens were notched by steel edges inserted before casting. No effects of structural segregation were observed in the neighbourhood of the notch tips. There were 9 beams (Fig. 3) and 7 prisms (Fig. 4) for each material.

The specimens were cured in water bath for 7 days and then stored in laboratory conditions with temperature $+18 \pm 2°C$ and 90% relative humidity for 21 days. At 28 days, the strength and fracture characteristics were determined using a ZD-10 GDR testing machine with a load controlling system.

The loading rate applied was $200\,N\,sec^{-1}$ and the load-displacement curves were recorded on a x–y plotter. Typical examples of the curves obtained are given in Figs 3 and 4.

5. Observation of the crack surfaces

In Fig. 5 a representative concrete specimen after rupture by shearing is shown. In all cases the final main crack started at one of the initial notches, and from the crack path it may be deduced that a true shearing failure occurred. New surfaces of the crack below the initial notch are shown in Fig. 6 and the following features may be observed: aggregate grains

TABLE I Values of K_{IIc}

Reference	Material	Specimen characteristic	K_{IIc} ($MN\,m^{-3/2}$)
[14]	Soil–cement	$a/W = 0.3$	0.42
		$a/W = 0.4$	0.41
		$a/W = 0.5$	0.43
[15]	Soil–cement	$a/W = 0.3$	0.42–0.43
		$a/W = 0.4$	0.41–0.42
		$a/W = 0.5$	0.43–0.44
[16]	Concrete with polypropylene fibres		0.48–0.55
	Concrete with steel fibres		0.44–0.60
[17]	Mortar 1 : 3, w/c = 0.45	$a = 35$ mm	1.76
		$a = 40$ mm	1.85
[18]	Mortar 1 : 3, w/c = 0.45	$a/W = 0.30$	1.86
		$a/W = 0.35$	1.75
		$a/W = 0.40$	1.78
		$a/W = 0.45$	1.78
[19]	Gravel concrete	max. grain	
	1 : 2.43 : 3.43 : 0.54	2–4	1.82
	$a/W = 0.4$	4–6.3	4.14
		6.3–8	3.56
		8–10	4.24
		10–12	3.85
		12–16	4.24
[20]	Gravel concrete	1 : 2.45 : 3.74 : 0.55	3.20
	$a/W = 0.4$	1 : 2.45 : 3.74 : 0.60	2.99
		1 : 2.45 : 3.74 : 0.65	2.86
		1 : 2.45 : 3.74 : 0.70	2.85
		1 : 2.45 : 3.74 : 0.75	2.29
		1 : 2.45 : 3.74 : 0.80	2.82
		1 : 2.45 : 3.74 : 0.85	2.11
		1 : 2.45 : 3.74 : 0.90	2.15
[21]	Basalt concrete 1 : 2.31 : 4.06 : 0.55	$a/W = 0.4$	4.45
	Gravel concrete 1 : 2.29 : 3.87 : 0.55		3.97
	Granite concrete 1 : 2.26 : 4.13 : 0.55		5.14
	Burned shale concrete 1 : 0.96 : 1.45 : 0.55		3.54

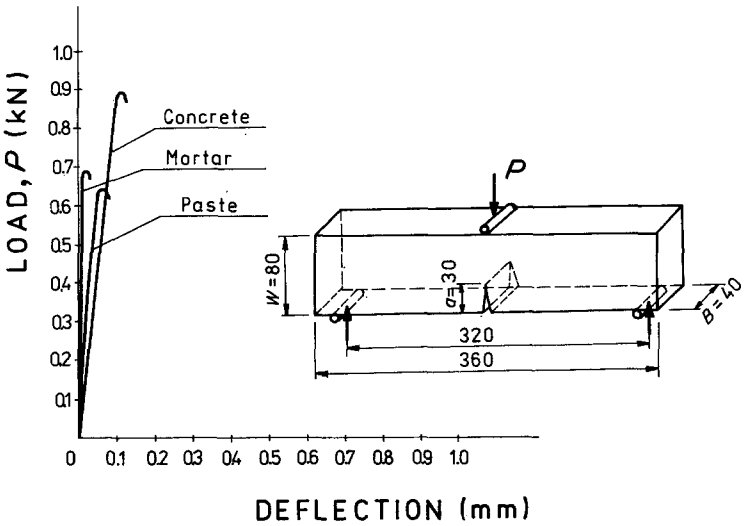

Figure 3 Examples of test results for K_{Ic} and dimensions of a notched beam subjected to bending.

(a), cracked grains (b), imprints due to grains pulled out (c) and macropores (d) in the mortar between grains.

Several observations have been made on micrographs obtained on small specimens sawn out after rupture from the regions around initial notches. The specimens were covered by graphite powder. The scanning electron microscope used was a Cambridge Scientific S4-10 with magnifications from $\times 50$ to $\times 2000$.

Example of micrographs are shown to illustrate the structure of cement paste (Figs 7 and 8), mortar (Figs 9 and 10) and concrete (Figs 11 and 12). In cement paste the most compact and homogeneous structure was observed with relatively few micropores or other microdefects. That homogeneity was certainly the reason for the particular brittleness of the neat cement paste specimens observed during tests. In cement mortar specimens, the microcracks appear between sand grains which represent only small obstacles easily contoured by propagating cracks. Numerous pores were observed between particles of C_3S close to sand grains. In the interface between sand grains and cement paste, discontinuities appeared, enabling small local displacements which resulted in quasi-plastic effects on load–displacement curves. The most numerous cracks and defects appeared in concrete specimens. Microcracks are visible in the interface layers between grains and cement paste, and also in cement paste itself. They were probably enhanced before loading in the processes of drying and shrinkage of the paste. The local displacements of grains and paste particles in cracked regions and subcritical crack formations were reflected in the load–displacement curves in the form of inflections, and these effects were clearer than on mortar specimens where there were far fewer defects. The quasi-plastic effects were not observed on cement paste specimens.

The material resistance against cracking is not only related to the strength of all components, but largely to the bond in all interfaces and to material defects which existed prior to loading. Various forms of these defects were observed on the micrographs.

6. Values of factors K_{Ic} and K_{IIc}

The critical values of stress intensity factors in modes I and II were determined according to ASTM formulae [22]

$$K_{Ic} = \frac{P_{cr}}{B\sqrt{W}} Y\left(\frac{a}{W}\right)$$

$$K_{IIc} = 5.11 \frac{P_{cr}}{2Bb} \sqrt{\pi a} \qquad (7)$$

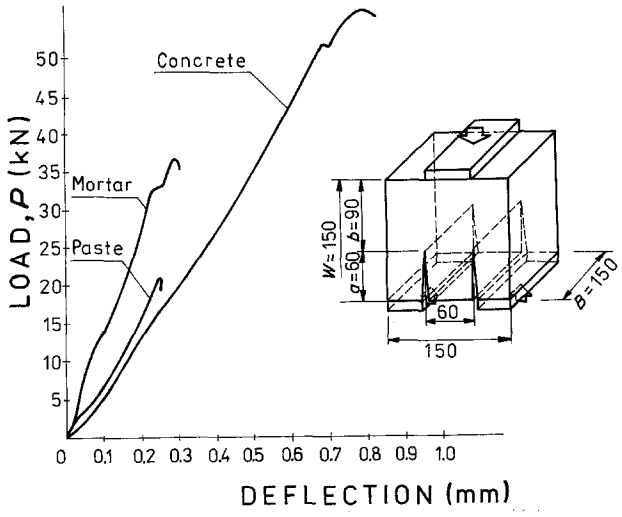

Figure 4 Examples of test results for K_{IIc} and dimensions of a punch-through shear specimen.

Figure 5 Concrete specimen after fracture by shearing in mode II.

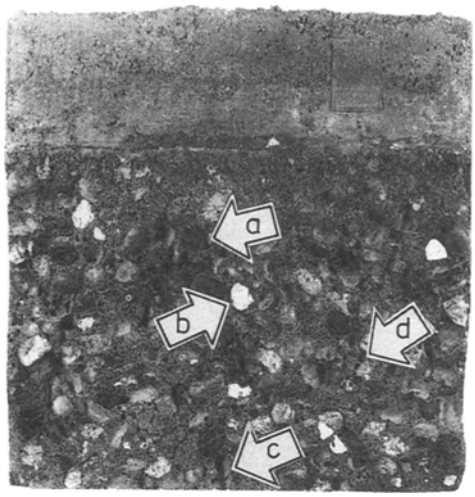

Figure 6 Crack surface below initial notch in a concrete specimen: (a) aggregate grains; (b) imprints of grains pulled out from matrix; (c) fractured grains; (d) micropores in the matrix.

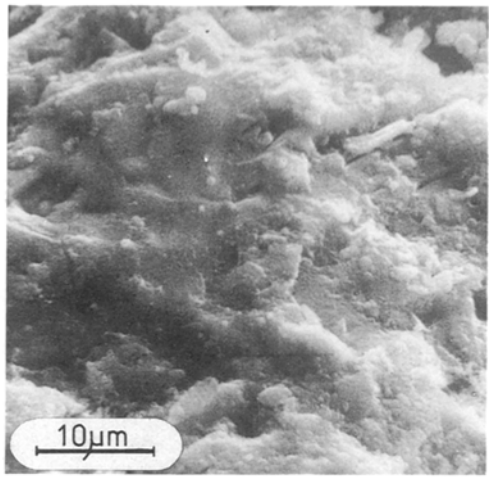

Figure 8 Brittle fracture across crystals in cement paste. The structure is compact and rather homogeneous. Magnification ×2000.

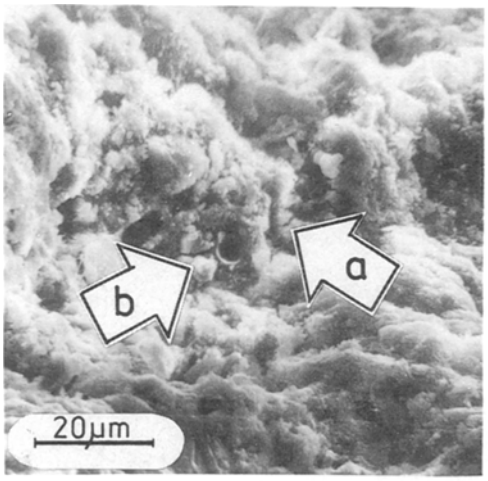

Figure 7 Brittle fracture in cement paste: (a) microcracks; (b) micropores in gel. Magnification ×1000.

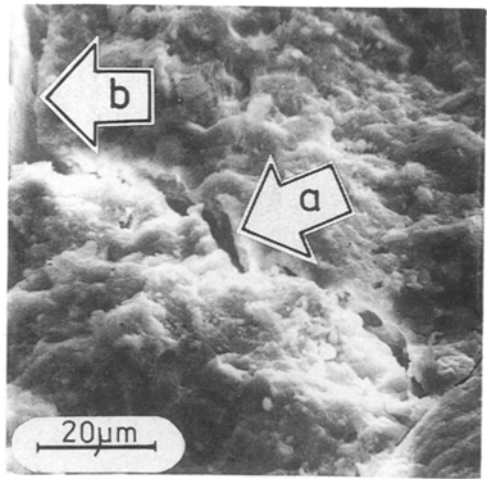

Figure 9 Microcrack in cement mortar between sand grains. The crack plane is perpendicular to grain faces (a). Discontinuities in the interface between grains and cement paste are visible (b). Magnification ×1000.

where P_{cr} is the value of the critical load P which initiated the crack propagation, W is specimen depth, b is ligament depth, a is notch depth and B is specimen width. That value of P_{cr} is identified on the curves (Figs 3 and 4) as a slight inflection for mode II curves or as maximum value for mode I curves.

The above formulae were proposed by ASTM and are applied here following Watkins [14] and others, although they were intended for application to metallic specimens. Therefore the obtained numerical results may be considered as only approximate. The question of the applicability of linear elastic fracture mechanics (LEFM) to relatively small specimens is beyond the scope of this paper. The values calculated from Equations 7 are presented in Table II.

The dispersion of the results obtained is particularly high for K_{IIc} and is probably related to the high influence of local crack resistance of the specimens. The highest values of the variation coefficient were observed for cement paste in both types of specimens.

TABLE II Test results

Parameter	Paste	Mortar	Concrete
Compressive strength (MPa)	56.9	30.5	35.3
coefficient of variation (%)	2.2	5.3	3.4
number of specimens	3	3	3
Critical value of stress intensity factor K_{Ic} (MN m$^{-3/2}$)	0.472	0.557	0.935
coefficient of variation (%)	13.2	7.5	4.3
number of specimens	9	9	9
Critical value of stress intensity factor K_{IIc} (MN m$^{-3/2}$)	1.480	2.430	3.648
coefficient of variation (%)	23.0	9.5	8.5
number of specimens	7	7	7

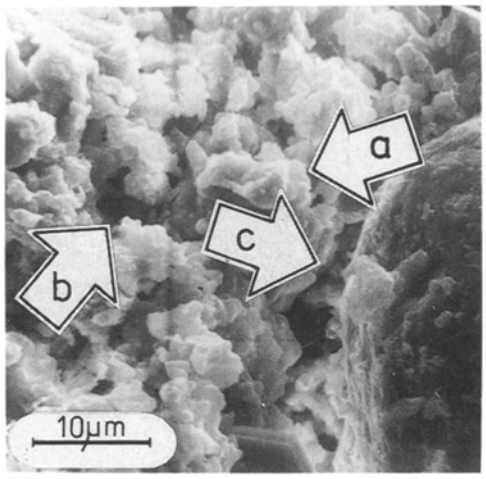

Figure 10 Brittle fracture across crystals in cement mortar. Particles of C_3S are visible (a), also pores in cement paste (b) and discontinuities in the interface between grain and cement paste (c). Magnification ×2000.

This result may be attributed to the relative homogeneity of that material structure and its brittleness. The cracks were not blocked by any inclusion and critical load was more related to random local defects at the crack path.

On the load–displacement plots for concrete and mortar specimens, a slight quasi-plastic effect in the form of inflections appeared (Fig. 4). This phenomenon may be related to rearrangement of the aggregate grains, after which an additional energy supply was required for further crack propagation. It was not observed on the curves for paste specimens.

The transgranular path of the cracks and their changes of direction when passing around the grains also require additional amounts of energy supplied by the external load. This was probably the reason why the higher values of fracture loads were necessary for concrete and mortar specimens than for paste ones.

It may be concluded that the results obtained confirm the data published previously by other authors. However, here the relations between K_{Ic} and K_{IIc} for the same materials have been discovered, which may be used in establishing a criterion for mixed-mode fracture in concretes.

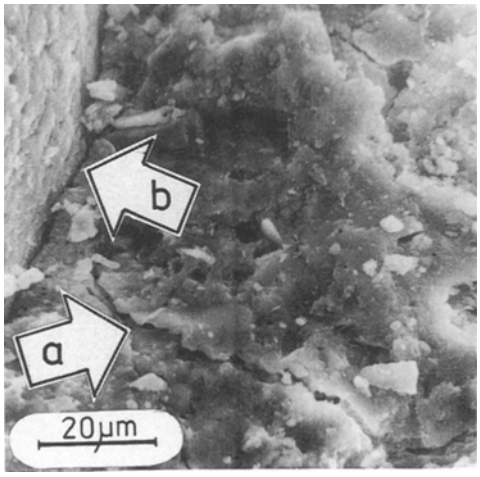

Figure 11 Concrete specimen. Brittle microcracks across paste (a) and between aggregate grain and cement paste (b). Magnification ×1000.

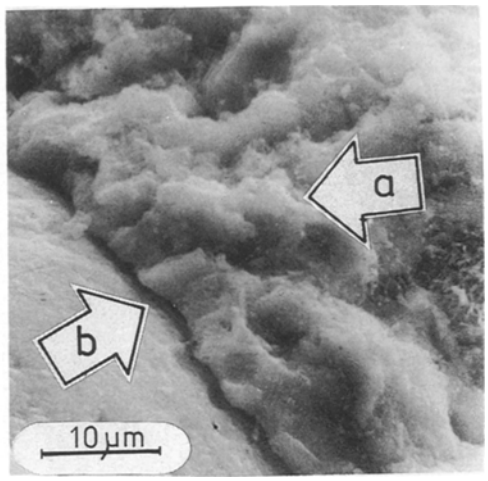

Figure 12 Concrete specimen. Brittle microcracks in cement paste (a) and in the interface between grain and paste (b). Magnification ×2000.

Acknowledgement

The research reported in this paper was supported by Project CPBP 02.01, item 1.4. coordinated by the Institute of Fundamental Technological Research in Warsaw.

References

1. M. F. KAPLAN, *J. American Concrete Institute* **58** (1961) 591.
2. J. GLUCKLICH, *J. Engng Mech. Div., Proc. ASCE* **89** (1963) 127.
3. D. BROEK, "Elementary Engineering Fracture Mechanics", (M. Nijhoff, The Hague, 1982).
4. S. MINDESS and S. DIAMOND, *Cement Concr. Res.* **10** (1980) 509.
5. S. MINDESS, in "Fracture Mechanics of Concrete", edited by F. H. Wittmann (Elsevier, Amsterdam, 1983) p. 1.
6. YU. V. ZAĬTSEV, A. A. ASHRABOV and M. B. KAZATSKI, in "Brittle Matrix Composites", vol. 1, edited by A. M. Brandt and I. H. Marshall (Elsevier Applied Science, 1986) p. 549.
7. G. DEBICKI, PhD Thesis, Institut National des Sciences Appliquées, Lyon, 1988.
8. G. S. SIH, *Int. J. Fract.* **10** (1974) 305.
9. J. G. WILLIAMS and P. D. EVING, *Int. J. Fract. Mech.* **8** (1972) 441.
10. G. C. SIH, P. C. PARIS and G. R. IRWIN, *ibid.* **1** (1965) 189.
11. G. C. SIH and E. P. CHEN, *J. Comp. Mater.* **7** (1973) 230.
12. G. T. HAHN, *Comp. Tech. Res.* **5** (1983) 26.
13. M. R'MILI, PhD Thesis, Institut National des Sciences Appliquées, Lyon, 1987.
14. J. WATKINS, *Int. J. Fract.* **23** (1983) R135.
15. J. DAVIES, T. G. MORGAN and A. W. YIM, *ibid.* **28** (1985) R3.
16. K. LIU, B. I. G. BARR and J. WATKINS, *Int. J. Cement Comp. Light. Concr.* **7** (1985) 93.
17. J. DAVIES and K. W. SO, *Int. J. Fract.* **31** (1986) R19.
18. J. DAVIES, *J. Mater. Sci. Lett.* **6** (1987) 879.
19. A. BOCHENEK and G. PROKOPSKI, *Archiwum Inżynierii Lądowej* **33** (1987) 359.
20. *Idem, Arch. Inż. Ląd.* **34** (1988) 261.
21. *Idem, ibid.* **35** (1989).
22. Standard Test Method in Plane Strain Fracture Toughness of Metallic Materials (ANSI/ASTM E 399-78, 1978).

Received 14 March
and accepted 30 August 1989